Chemical composition, in vitro color reconstruction, and bee vision modeling regarding anthocyanins and other phenolics from the flowers of Petrea macrostachya and Petrea volubilis

Qi Qin

s245225w@st.go.tuat.ac.jp

Tokyo University of Agriculture and Technology: Tokyo Noko Daigaku https://orcid.org/0009-0005-1320-666X

Shinnosuke Mori

Keio University - Hiyoshi Campus: Keio Gijuku Daigaku - Hiyoshi Campus

Ayako Nishikawa

Mito Botanical Park

Fumi Tatsuzawa

Iwate University: Iwate Daigaku

Takahisa Nakane

Showa Pharmaceutical University: Showa Yakka Daigaku

Tsukasa Iwashina

National Museum of Nature and Science: Kokuritsu Kagaku Hakubutsukan

Takayuki Mizuno

National Museum of Nature and Science: Kokuritsu Kagaku Hakubutsukan

Research Article

Keywords: Bee hexagon model, Color intensity, Petrea macrostachya, Phenolic acids, Vanilloyl delphinidin glycoside

Posted Date: August 25th, 2025

DOI: https://doi.org/10.21203/rs.3.rs-7296548/v1

Version of Record: A version of this preprint was published at Journal of Plant Research on June 10th, 2026. See the published version at https://doi.org/10.1007/s10265-026-01724-1.

Abstract

Delphinidin 3-*O*-[6-(4-*O*-(6-(4-*O*-*β*-glucopyranosylvanilloyl)-*β*-glucopyranosyl)-vanilloyl)-*β*-glucopyranoside]-5-*O*-*β*-glucopyranoside (petreadelphin), a novel anthocyanin, and *β*-(3,4-dihydroxyphenyl)ethyl 4-*E*-caffeoyl-3,6-di-*β*-xylopyranosylglucopyranose (petreathanoside), a novel phenylethanoid, were respectively isolated from the violet petals and sepals of *Petrea macrostachya* (Verbenaceae). In addition, nine known phenolic compounds were also isolated from the tepals of *P. macrostachya*.

The pH of the petals and sepals was shown to be 5.7 and 5.6, respectively. *In vitro* color reconstruction experiments using two anthocyanins, namely, petreadelphin from the petals and delphinidin 3-*O*-(6-caffeoylglucoside)-5-*O*-glucoside from the sepals, revealed that their absorption spectra closely match those of the corresponding floral tissues. We also found that these anthocyanins are primarily responsible for the coloration of the petals and sepals.

Stability assays showed that the sepal anthocyanin faded rapidly after 15 min in the buffer solution, whereas petreadelphin retained its color for at least 24 hours. This is attributed to the greater structural stability of petreadelphin conferred by its polyacylation.

In addition, bee color vision modeling using the reflectance spectra indicated that the petals have significantly higher color intensity than sepals. These findings suggest that the type and number of acyl groups in anthocyanin may enhance pigment stability and light absorption, thereby contributing to increased intensity and potentially improving floral detectability by bees.

Introduction

The *Petrea* (Verbenaceae) genus comprises 14 species, three of which are known only from fossils. The extant species are distributed throughout the Neotropical region, ranging from southern Mexico through Central America and the West Indies to Bolivia, Paraguay, and Brazil, with the highest diversity and concentration occurring in northern Brazil and the Guianas (Rueda 1994). Among them, *P. macrostachya* Benth. is endemic to Guyana, French Guiana, and Suriname. The most widely distributed species in the genus is *P. volubilis* L., which ranges from the southern half of Mexico and the West Indies to Peru and Paraguay (Rueda 1994). *Petrea*, commonly known as the queen's wreath or sandpaper vine, is characterized by its terminal clusters of flowers and rough, scabrous leaves.

The leaves of *P. volubilis* have traditionally been used for the treatment of diabetes (Rahman et al. 2010), as well as for burns, wounds, inflammation, and abscesses (Abdelwahab et al. 2011). Several studies have investigated its chemical constituents and identified various flavonoids such as apigenin, quercetin, and pectolinarigenin, along with organic acids such as hypogallic acid, *trans*-caffeic acid, vanillic acid, acteoside, eukovoside, and cistanoside D (Abdelwahab et al. 2011; Dawoud and El-Morsy 2012).

Although some *Petrea* species exhibit striking violet petals and sepals, the pigments responsible for these colors have not been characterized to the best of our knowledge. Moreover, it remains unclear whether there are differences in pigment structure and composition between petals and sepals, and how such differences might influence pollinator perception.

To address these questions, we isolated and identified the pigments from the petals and sepals of *P. macrostachya*. In addition, the floral pigments of *P. volubilis* were characterized by HPLC comparison with those of *P. macrostachya*. To identify the compounds responsible for coloration, we conducted *in vitro* color reconstruction experiments using the isolated pigments. The pH of the petals and sepals was also measured to enable reconstruction under physiologically relevant pH conditions.

Since flower color plays a key role in pollinator attraction, we further examined the potential signaling function of petal and sepal coloration in a pollination system. Euglossini bees have been reported as the primary pollinators of *Petrea* flowers, with additional visits observed from introduced *Apis* and *Bombus* species, as well as Heliconiidae butterflies (Rueda 1994). We evaluated whether and how petal and sepal coloration in *Petrea* species may function as visual cues for bee pollinators, using visual modeling based on reflectance spectra.

Materials and methods

Plant material

Fresh flowers of *P. macrostachya* (27.19 g of petals and 52.40 g of sepals) and *P. volubilis* (6.33 g of petals and sepals combined) were collected from Mito Botanical Park (Ibaraki, Japan) on June 3, 2023. Color measurements, pH measurements, and HPLC analyses were performed on both *P. macrostachya* and *P. volubilis*, while pigment isolation was conducted exclusively on *P. macrostachya*.

Isolation and identification of anthocyanins and other phenolics

Fresh petals and sepals of *P. macrostachya* were extracted for one day using 5% HCOOH in MeOH. After evaporation, the petal extracts were applied to a Diaion HP-20SS column chromatography (Mitsubishi Chemical, Japan) and eluted with 280 mL 0.5% TFA aq., 280 mL 10% MeCN containing 0.5% TFA, and 280 mL 25% MeCN containing 0.5% TFA. The sepal extracts were applied to a C-850 flash chromatography (Büchi, Switzerland) using FP SELECT C18 12 g column (Büchi).

The separated fractions were applied to preparative HPLC with a Shimadzu HPLC system equipped with an SPD-20A UV-vis detector using Inertsil ODS-4 (5-μm particle material, I.D. 10 × 250 nm, GL Sciences, Inc.). The chromatographic conditions were as follows: a flow rate of 3.0 mL min^{-1}, detection at 530 nm for anthocyanins and at 350 nm for other phenol components, and an eluent of 10–25% MeCN containing 5% HCOOH. Fractions were further purified using Sephadex LH-20 gel filtration chromatography eluting with 70% MeOH aq. containing 5% HCOOH.

Isolated compounds were identified using UV-vis spectroscopy, LC-MS, NMR, and HPLC. UV-vis spectra were recorded on a UV-2600 spectrophotometer (Shimadzu) following the approach of Mabry et al. (1970). LC-MS was performed with a Shimadzu LC-MS system equipped with an SPD-20A UV-Vis detector (190–700 nm) using Inertsil ODS-4 (3-μm particle material, I.D. 2.1 × 100 mm, GL Sciences, Inc.) at a flow rate of 0.2 mL min^{-1}, eluted with 7–25% MeCN containing 5% HCOOH, ESI^+ 4.5 kV and ESI^- 3.5 kV, at the interface temperature of 250°C. Anthocyanin **A1** was identified by NMR [JEOL ECZ400S in CD_3OD–TFA (9:1) in TMS as 0 ppm, 400 MHz ^1H NMR, and 100 MHz ^{13}C NMR] including ^1H NMR, ^{13}C NMR, HMQC, HMBC, COSY, NOESY, and TOCSY. Phenolics **P2**, **P4**, and **P6** were measured by NMR [Bruker AV-600 in DMSO-d_6 at 600 MHz ^1H NMR and 150 MHz ^{13}C NMR] including ^1H NMR, ^{13}C NMR, HSQC, HMBC, COSY, and NOESY. Fast atom bombardment mass spectrometry (FAB-MS) analysis of **A1** was obtained in positive ion mode with a JMS-700 system (JEOL Ltd., Tokyo, Japan) using the magic bullet (5:1 mixture of dithiothreitol and dithioerythritol) as a matrix. **P1**–**P3**, **P5**–**P7**, and **F1**–**F2** were compared with authentic samples by HPLC retention times. The origins of the authentic samples used were as follows: *E*-caffeoylglucose from *Primula sieboldii* É. Morren flowers (Hashimoto et al. 2015), E-feruloylglucose from *Hedychium coronarium* J. Koenig flowers (Murakami et al., unpublished data), acteoside and plantamajoside from *Aeschynanthus* cultivars flowers (Iwashina et al. 2022), luteolin 7-*O*-glucuronide from *Myoporum bontioides* (Siebold & Zucc.) A. Gray flowers (Iwashina and Kokubugata 2010), and apigenin 7-*O*-glucuronide from *Aeginetia indica* L. flowers (Iwashina 2010).

Deacylation and acid hydrolysis

Deacyl treatment of authentic delphinidin 3-*O*-(6-caffeoylglucoside)-5-*O*-(6-malonylglucoside) from the petals of *Salvia splendens* 'Flamenco Purple' (Seto et al. 2022) was performed by the addition of 2 M HCl. The mixture was left at room temperature for one week (Qin et al. 2024) and injected into HPLC to compare with the retention time of **A2**. **A1** was hydrolyzed in 500 μL 95% MeOH containing 5% HCOOH, followed by the addition of 1 mL 2 N HCl aq., 100°C, 30 min. After cooling, hydrolysate was separated using a Sep-Pak Plus Light C18 (Waters, USA). The fraction containing aglycone was characterized by HPLC comparison with authentic cyanidin, delphinidin, and pelargonidin (Tokiwa Phytochemical Co., Ltd., Japan).

Sugar analysis

A1 was dissolved in 2 mL 0.5 M HCl and heated at 100°C for 40 min. After cooling, hydrolysate was filtered through a Sep-Pak Plus Light C18 (Waters). The fraction was neutralized by a WAX column (Waters Co.). Aldoses were analyzed following the approach of Tanaka et al. (2007). The residue was dissolved in 50 μL pyridine containing L-cysteine (10 mg mL^{-1}) and heated at 60°C for 60 min. Phenylisothiocyanate (10 mg mL^{-1}) of 50 μL was then added to the mixture and heated at 60°C for 60 min. The resulting derivatives were compared to authentic aldose reaction products by HPLC comparison (Mizuno et al. 2021). HPLC analysis was performed with a Shimadzu HPLC system equipped with an SPD-20A UV-vis detector using Cosmosil 5C18-AR-II (5-μm particle material, I.D. 4.6 × 250 nm, Nacalai Tesque, Inc., Japan).

HPLC comparison between P. macrostachya and P. volubilis

Fresh petals and sepals (0.2 g) of *P. macrostachya* and *P. volubilis* were extracted for one day with 4 mL of 70% MeOH aq. containing 5% HCOOH for HPLC analysis. The extracts (10 µL) were injected into a Shimadzu HPLC system equipped with an SPD-20A UV-vis detector using InertSustain AQ-C18 (5-µm particle material, I.D. 4.6 × 250 mm, GL Sciences) at a flow rate of 1.0 mL min^{-1}. Solvents A (5% HCOOH aq.) and B (90% MeCN aq., 5% HCOOH) were used for the mobile phase under a linear gradient condition from 10 to 50% solvent B for 35 min, and 50% solvent B for 10 min.

Measurement of the color and pH

The colors of the petals and sepals were surveyed by comparison with the RHSCC sixth edition, and their CIE L*a*b* chromaticity values were measured using a CR-10 color reader (Konica Minolta, Inc. Japan). The absorption spectra of the petals and sepals of *P. macrostachya* were directly measured using a UV-2600 spectrophotometer (Shimadzu) equipped with an integrating sphere ISR-2600 (Shimadzu) and transmitted light. The pH of the petal and sepal pressed juice of *P. macrostachya* and *P. volubilis* was measured using a twin pH meter AS-212 (HORIBA Ltd., Japan) in triplicate, and the average value was calculated.

In vitro reconstruction of petal and sepal colors

The anthocyanins isolated from the petals and sepals of *P. macrostachya* were lyophilized. McIlvaine buffers were adjusted to pH 5.7 and 5.6, corresponding to the average pH values of the petals and sepals, respectively. Buffer solutions containing 1 mM **A1** and **A2** were prepared. Spectra were measured using a UV-2600 spectrophotometer (Shimadzu). Each sample solution was loaded into a Nano Stick-S microcell (Scinco, Korea), and absorbance was recorded over the wavelength range of 400–700 nm (Mizuno et al. 2021). The absorption spectra of 0.1 mM **A1** at pH 5.6 and **A2** at pH 5.7 were recorded to investigate whether the slight pH difference (0.1) between the petals and sepals contributes to their color variation. At these pH conditions corresponding to petals and sepals of *P. volubilis*, the absorption spectra were compared with those of its intact petals and sepals. Additionally, the color stability of **A1** and **A2** at a pH 5.7 buffer solution was evaluated by photographing the samples immediately after measurement, after 15 min, and after one day.

Visual model of bees and color variables

The reflectance spectra (300–700 nm) of *P. macrostachya* petals and sepals were measured using a UV-2600 spectrophotometer (Shimadzu) equipped with an integrating sphere (ISR-2600). Barium sulfate (Ba_2SO_4) powder was used as the white reference standard. Since the photopigments underlying trichromatic vision are conserved in Hymenoptera, the spectral sensitivity of the western honeybee (*Apis mellifera* L.) was applied to model bee vision, the primary floral visitors of *Petrea* (Peitsch et al. 1992; Rueda 1994). The color loci of *P. macrostachya* petals and sepals were calculated and plotted in the bee color hexagon (Chittka 1992) in *RStudio* (version 2024.04.2, Build 764) using the pavo package (Maia et

al. 2013). The averaged leaf reflectance spectrum provided in pavo was set as the background. The CIE D65 daylight irradiance spectrum was used as the standard model for daylight illumination.

Bee achromatic contrast was determined as the absolute difference |0.5 − *E*(G)|, following the method of Spaethe et al. (2001), where *E*(G) represents the green receptor excitation. Bee chromatic contrast was quantified as the Euclidean distance between the tepal locus and the hexagon center in the bee color space, as described by Chittka (1992). Color intensity was calculated as the total sum of photoreceptor excitations across all receptor types, following Spaethe et al. (2001). Spectral purity was measured as the ratio of the distance between the stimulus locus and the hexagon center to the distance between the stimulus locus and the nearest spectrum locus, as defined by Lunau et al. (1996). To evaluate whether bees could distinguish between petal and sepal colors of *P. macrostachya*, the color distances between all combinations of four petal and five sepal measurements in the hexagon color space were calculated.

Data for novel anthocyanin and phenolic acid

Delphinidin 3-*O*-[6-(4-*O*-(6-(4-*O*-glucosylvanilloyl)-glucosyl)-vanilloyl)-glucoside]-5-*O*-glucoside (**A1**, petreadelphin). TLC: Rf 0.20 (BAW), 0.04 (BuHCl), 0.20 (1% HCl), 0.49 (AHW). UV-vis: λ_{max} (nm): 0.01% HCl–MeOH 249, 350, 553; $E_{acyl(249)}/E_{max}$ 85%; E_{440}/E_{max} 7%; +$AlCl_3$ bathochromic shift. HR-MS (ESI): $[M]^+$ Calc. for $C_{55}H_{63}O_{33}^+$: 1251.3251, Found: 1251.3219 ($C_{55}H_{63}O_{33}^+$). ^1H and ^{13}C NMR: see Table 1.

β-(3,4-dihydroxyphenyl)ethyl 4-*E*-caffeoyl-3,6-di-*β*-xylopyranosylglucopyranoside (**P4**, petreathanoside). UV-vis: λ_{max} (nm): MeOH 292, 336. LC-MS: *m/z* 765.2226 $[M + Na]^+$, 741.2220 $[M - H]^-$. ^1H and ^{13}C NMR: see Table 2.

Results

Identification of anthocyanins and other phenolics

Two anthocyanins (**A1** and **A2**), seven organic acids (**P1**–**P7**), and two flavones (**F1**–**F2**) were isolated from the petals and sepals of *P. macrostachya*. Among them, **A1** and **P4** are identified for the first time as natural products. Their chemical structures are shown in Figs. 1 and 2.

Acid hydrolysis of **A1** liberated delphinidin, which was subsequently characterized by HPLC comparisons with authentic samples. Glycosidic sugar was determined to be D-glucose by HPLC analyses after the thiocarbamoyl-thiazolidine derivatization. HR/MS showed a molecular ion peak at *m/z* 1251.3219 $[M]^+$, indicating that delphinidin is conjugated with two additional moieties of 168 Da each, along with four glucose residues. In the ^1H NMR, ten aromatic and two methoxy proton signals occurred. Among them, four signals (δ_H 8.72, 7.54, 7.13, and 6.81) were assigned to H-4, H-2′, H-6′, H-6, and H-8 of delphinidin (Table 1 and Fig. S1). The remaining six aromatic proton signals (δ_H 7.57, 7.54, and 6.81, and 7.20, 6.58, and 6.37) corresponded to H-2, H-6, and H-5 of vanillic acid. Two methoxy proton signals at δ_H 3.88 and 3.58 showed HMBC correlations with C-3 carbon signals of vanillic acid at δ_C 150.7 and 150.0,

respectively (Fig. S3). These results indicate that the two additional moieties were vanillic acid, which has been found in the leaves of *P. volubilis* (Abdelwahab et al. 2011). Among four glucosyl anomeric proton signals, two (δ_H 5.65 and 5.03) were correlated with C-3 (δ_C 146.7) and C-5 (δ_C 156.6) signals of delphinidin, respectively, in HMBC, and two (δ_H 5.00 and 5.23) were correlated with C-4 signals of vanillic acid at δ_C 152.2 and 151.2, respectively. The HMBC spectra revealed key correlations between δ_C 152.2 (Van-a C-4) and δ_H 5.02 (Glu-C H-1), and between δ_C 151.2 (Van-b C-4) and δ_H 5.23 (Glu-D H-1) (Fig. S3). Furthermore, the C-6 of Glu-A (δ_C 66.2) and Glu-C (δ_C 66.5) shifted to the lower field. Based on these results, **A1** was identified as delphinidin 3-*O*-[6-(4-*O*-(6-(4-*O*-glucosylvanilloyl)-glucosyl)-vanilloyl)-glucoside]-5-*O*-glucoside, and named as petreadelphin (Fig. 1). Another anthocyanin, **A2**, was identified as delphinidin 3-*O*-(6-caffeoylglucoside)-5-*O*-glucoside (Fig. 3) by UV-vis spectral properties, LC/MS, and HPLC comparison with a deacylated authentic sample. This anthocyanin from the genus *Petrea* is identified here for the first time.

^{1}H NMR, ^{13}C NMR, and LC/MS data of **P4** suggest that it consists of a phenylethyl moiety, a *trans*-caffeoyl moiety, and three sugar units: one glucosyl and two xylosyl. The presence of the 3,4-dihydroxyphenylethyl moiety was confirmed by characteristic carbon signals at δ_C 70.1 and 34.9. The *trans*-caffeoyl moiety was characterized by the occurrence of two doublet signals at δ_H 7.46 (d, J = 16.2 Hz) and 6.22 (d, J = 16.2 Hz), corresponding to the *trans*-configuration of the double bond, along with a carboxyl carbon signal at δ_C 165.8 (Table 2). The glycosyl unit was characterized based on the anomeric proton signal at δ_H 4.40 (d, J = 7.8 Hz), which exhibited an HMBC correlation with δ_C 70.1 (Dih C-α), confirming its glycosidic linkage to the phenylethanoid moiety (Fig. S7). The presence of two xylosyl units was confirmed by two additional anomeric signals at δ_H 4.30 (X H-1) and 4.14 (X H-1), which showed HMBC correlations with δ_C 83.8 (Glu C-3) and 67.8 (Glu C-6), respectively (Fig. S7). From these results, **P4** was identified as *β*-(3,4-dihydroxyphenyl)ethyl 4-*E*-caffeoyl-3,6-di-*β*-xylopyranosylglucopyranose (Fig. 2).

The other six phenolic acids and two flavones were characterized as *E*-caffeoylglucose (**P1**), neochlorogenic acid (**P2**), *E*-feruloylglucose (**P3**), plantamajoside (**P5**), forsythoside F (**P6**), acteoside (**P7**), luteolin 7-*O*-glucuronide (**F1**), and apigenin 7-*O*-glucuronide (**F2**). Their chemical structures are shown in Fig. 3. Among them, **P2** and **P6** were identified by UV-vis spectra, LC/MS, and NMR. Other compounds were characterized by UV-vis spectra, LC/MS, and HPLC comparisons with authentic samples. These phenolic acids and flavones from the *Petrea* species are reported here for the first time, except for acteoside, which has been found from *P. volubilis* leaves (Abdelwahab et al., 2011; Dawoud and El-Worsy, 2012).

The chemical compositions of the petals and sepals of *P. macrostachya* and *P. volubilis* were analyzed by HPLC (Fig. S13). Among the compounds found in this study, **A1** was detected exclusively in the petals of both species, while **A2** was detected exclusively in the sepals. Although most compounds were present in both petals and sepals, acteoside (**P7**) was a major compound in *P. macrostachya*. Two flavones, **F1** and **F2**, were detected in the petals and sepals of both species.

Petal and sepal colors and their pH

Petals and sepals of both *P. macrostachya* and *P. volubilis* were classified into the VIOLET group (Table 3) according to the RHSCC (Royal Horticultural Society Colour Chart, sixth edition). Among the measured samples, the petals of *P. macrostachya* exhibited the lowest b* value (− 23.9 ± 4.0), indicating the strongest blue tone. The absorption maxima (λ_{max}) of the petals and sepals are presented in Table 3. The absorption spectra of *P. macrostachya* petals and sepals were similar to those of *P. volubilis*. The petal spectra exhibited two absorption maxima within the 530–570 nm range, along with a shoulder near 624 nm, whereas the sepal spectra showed two absorption maxima within the 540–570 nm range, along with a shoulder near 624 nm. The petal pH of *P. macrostachya* was 5.7, while its sepal pH was 5.6. *P. volubilis* showed the opposite trend, with a petal pH of 5.6 and a sepal pH of 5.7.

In vitro reconstruction of petal and sepal color

The absorption spectra of intact petals and sepals of *P. macrostachya* are shown in Fig. 4, together with those of reconstructed solutions containing **A1** or **A2**. The absorption maxima of the petals were observed at 537.6 and 568.0 nm, with a shoulder at 624.0 nm, while the reconstructed solution of **A1** at pH 5.7 exhibited absorption maxima at 535.6 and 570.2 nm, with a shoulder at 617.2 nm. The absorption maxima of the sepals were 549.8 nm and 565.0 nm, with a shoulder at 624.6 nm, and the reconstructed solution of **A2** at pH 5.6 showed an absorption maximum at 546.2 and 570.2 nm. The absorption spectra of the reconstructed solutions closely matched those of the corresponding floral parts (Fig. 4). The absorption spectra of the *P. volubilis* petal and sepal were also reconstructed using **A1** in pH 5.6 and **A2** in pH 5.7, respectively. The absorption curves of the solutions were similar to the shape of corresponding flower parts (Fig. S14). Even after one day, **A1** in buffer solution retained its deep violet color, whereas **A2** faded to near-colorless under the same buffer condition (Fig. S15).

Spectral reflectance and bee visual perception

The reflectance spectra of *P. macrostachya* petals and sepals are shown in Fig. 5. The color loci of *P. macrostachya* petals and sepals in the bee color space are shown in Fig. 6 (see also Table S3 for detailed data). Based on the bee hexagon model, the petal color loci were positioned between the Blue and UV-Blue categories, while the sepal color loci were classified as Blue (Fig. 6). No significant differences were found between petals and sepals in terms of chromatic contrast, achromatic contrast, and spectral purity ($p > 0.05$). However, a significant difference was observed in intensity, with petals exhibiting higher intensity than sepals ($p < 0.05$, Fig. 7). The Euclidean distances between all combinations of four petal and five sepal measurements in the hexagon color space are shown in Table 4. Distances ranged from 0.093 to 0.130 hex units (mean ± SD: 0.113 ± 0.009).

Discussion

In this survey, two anthocyanins, seven phenolic acids, and two flavones were isolated and identified from the flowers of *Petrea macrostachys* and *P. volubilis*. Among them, one anthocyanin and one

phenolic acid were previously unreported compounds in nature and were named petreadelphin and petreathanoside, respectively. The chemical structure of petreadelphin is notable for the presence of vanilloyl moieties. Although aromatic acyl groups such as *p*-coumaroyl, caffeoyl, feruloyl, sinapoyl, and 3,5-dihydroxycinnamoyl have been reported as common anthocyanin modifications (Zhao et al. 2017), vanilloyl moiety is rarely observed in anthocyanins.

He et al. (2016) isolated two anthocyanins from purple-fleshed sweet potatoes and tentatively characterized them as cyanidin 3-caffeoyl-vanilloyl sophoroside-5-glucoside and peonidin 3-caffeoyl-vanilloyl sophoroside-5-glucoside using UPLC-PDA and UPLC-QTOF-MS/MS. However, as far as we know, petreadelphin is the first vanilloyl-conjugated anthocyanin identified by NMR.

Petreathanoside was identified as a novel phenylpropanoid structurally related to forsythoside F, with a xylosyl group replacing a rhamnosyl group. Phenylethanoid compounds such as acteoside, eukovoside, and cistanoside D have previously been reported in the leaves of *P. volubilis* (Dawoud and El-Morsy 2012). In the present study, phenylethanoid compounds **P4**–**P7** were also identified, suggesting the potential medicinal value of the tepals of *P. macrostachya*.

The petal and sepal colors of both species were classified into the VIOLET group according to the RHSCC. However, the petals of both species were assigned to the A chip, while the sepals were assigned to the D chip (Table 3). Since the RHSCC arranges colors from A (full color) to D (lightest) (Voss 2002), this indicates that the sepals are significantly lighter, as also supported by the L* values (Table 3).

The extracts from the petals and sepals of *P. macrostachya* exhibited similar profiles for compounds detected at 350 nm, while anthocyanins detected at 530 nm differed markedly (Fig. S13). This suggests that the color differences are largely attributed to differences in anthocyanin composition: **A1** predominates in petals, while **A2** is predominant in sepals. In addition, **A1** and **A2** were also detected in the petals and sepals of *P. volubilis*, respectively (Fig. S13), further supporting their functional roles in floral color differentiation. The absorption spectra of reconstructed solutions using the major anthocyanins closely matched those of the corresponding intact floral parts. This indicates that the colors of the petals and sepals of *P. macrostachya* are primarily determined by the color of predominant anthocyanin in each part, which is consistent with the HPLC results (Fig. S13). Furthermore, the pH difference of 0.1 between the petals and sepals did not affect their absorption spectra (Fig. 4 and Fig. S14).

As shown in Fig. S15, **A1** remained violet even after one day, presumably due to its acyl groups and its long chain-like structure. It has been reported that the acylation of anthocyanin glycosides can significantly enhance their resistance to various factors (Zhao et al. 2017). Other chain-like anthocyanins such as bicolmalonin, i.e., cyanidin 3-*O*-(4,6-di-*O*-malonylglucoside)-7-*O*-[6-*E*-(4-*O*-(6-*E*-caffeoylglucosyl)-caffeoyl)-glucoside]-3'-*O*-[6-*E*-caffeoylglucoside], which was isolated from the leaves of *Gynura bicolor* DC, have shown high antioxidative activities (Shimizu et al. 2010). Additionally, ternatins from the flowers of *Clitoria ternatea* L. have demonstrated heat stability in acidic pH (Vidana Gamage et al. 2021). Given

the health benefits of anthocyanins and the structural stability of **A1**, it has the potential to be a promising natural food colorant.

The bee visual modeling revealed that the petals and sepals of *P. macrostachya* occupy distinct positions in the bee color space: petal loci were located between the Blue and UV-Blue sectors, while sepal loci fell within the Blue sector. The color distance between petals and sepals (0.113 hex units) slightly exceeds the discrimination threshold of 0.1 (Chittka et al. 1993), suggesting that bees may be capable of distinguishing between them, albeit subtly. While no significant differences were detected in chromatic contrast, achromatic contrast, or spectral purity between petals and sepals, a significant difference was found in intensity, with petals exhibiting higher values. This difference might be attributed to chemical differences between petals and sepals, largely reflecting variation in their major anthocyanins **A1** vs. **A2**. Moreover, the chromatic contrast values for both petals and sepals exceeded 0.1 (0.156 ± 0.011), implying that both organs are detectable against green foliage and thus can function as visual signals for bee pollinators. Since larger floral displays are known to enhance bee attraction (Makino et al. 2007), sepals may contribute visually by expanding the perceived floral size. Further behavioral assays are needed to empirically assess the role of sepal coloration in pollinator attraction.

The structural basis of intensity differences between petals and sepals may lie in anthocyanin modification. Chemical analyses revealed that the main anthocyanin in the petals was delphinidin 3-*O*-[6-(4-*O*-(6-(4-*O*-glucosylvanilloyl)-glucosyl)-vanilloyl)-glucoside]-5-*O*-glucoside, while sepals primarily contained delphinidin 3-*O*-(6-caffeoylglucoside)-5-*O*-glucoside. Both pigments share a delphinidin 3,5-di-*O*-glucoside core, but the petal anthocyanin has more acyl modifications. These structural differences, particularly the type and number of acyl groups, may enhance anthocyanin stability and light absorption, thereby contributing to the deeper coloration and higher intensity observed in the petals.

Conclusion

This study elucidated the floral color characteristics and chemical compositions of *P. macrostachya*, focusing on differences between petals and sepals. Our chemical analyses revealed that the color differences are primarily underpinned by structural differences in the major anthocyanins, **A1** and **A2**, particularly in their acylation patterns. Spectral reflectance measurements and bee vision modeling further demonstrated that petals and sepals differ in their perceptual properties as viewed by bees. The color distance between petals and sepals exceeded the discrimination threshold, suggesting that bees are capable of distinguishing between them, albeit subtly. In addition, the chromatic contrast values of both petals and sepals exceeded 0.1, indicating that both organs are visually detectable against a green foliage background and may function as floral clues. While no significant differences in chromatic contrast, achromatic contrast, or spectral purity were found, the significantly higher intensity observed in the petals may enhance their visual salience within the inflorescence. These findings highlight the integrated role of pigment chemistry and optical properties in shaping the visual signaling of floral organs in *Petrea*. Nevertheless, further behavioral studies under natural conditions are necessary to fully understand the ecological significance of sepal coloration in pollinator attraction.

Declarations

Competing Interests

The authors have no conflict of interest directly relevant to the content of this article.

References

1. Abdelwahab MF, Abdel-Lateff A, Fouad MA, Desoukey SY, Kamel MS (2011) Phytochemical and biological study of *Petrea volubilis* L. (Verbenaceae). Bulletin of Pharmaceutical Sciences Assiut University 34:9–20
2. Chittka L (1992) The colour hexagon: a chromaticity diagram based on photoreceptor excitations as a generalized representation of colour opponency. J Comp Physiol A 170:533–543. https://doi.org/10.1007/BF00199331
3. Chittka L, Vorobyev M, Shmida A, Menzel R (1993) Bee colour vision: the optimal system for the discrimination of flower colours with three spectral photoreceptor types. Sensory systems of arthropods 211–218
4. Dawoud GT, El-Morsy TH (2012) Phytochemical and microbiological studies of *Petrea volubilies* L. J American Science 8:202–208
5. Hashimoto N, Ohsawa R, Kitajima J, Iwashina T (2015) New Flavonol Glycosides from the Leaves and Flowers of *Primula sieboidii*. Natural Product Communications 10:421–423. https://doi.org/10.1177/1934578x1501000311
6. He W, Zeng M, Chen J, Jiao Y, Niu F, Tao G, Zhang S, Qin F, He Z (2016) Identification and Quantitation of Anthocyanins in Purple-Fleshed Sweet Potatoes Cultivated in China by UPLC-PDA and UPLC-QTOF-MS/MS. J Agric Food Chem 64:171–177. https://doi.org/10.1021/acs.jafc.5b04878
7. Iwashina T (2010) Flavonoids from two parasitic and achlorophyllous plants, *Aeginetia indica* and *Orobanche minor* (Orabanchaceae). Bulletin of the National Museum of Nature and Science, Series B 36:127–132
8. Iwashina T, Kokubugata G (2010) Flavonoids in the leaves and flowers of *Myoporum bontioides* native to northernmost region in the *Myoporaceae*. Bull Natl Sci Mus Ser B 36:117–125
9. Iwashina T, Rahayu S, Nakane T, Devkota HP, Mizuno T, Tsutsumi C, Widyatmoko D (2022) Flavonoids and phenylethanoids from the flowers and leaves of *Aeschynanthus* species and cultivars (Gesneriaceae). Phytochemistry 203:113367. https://doi.org/10.1016/j.phytochem.2022.113367
10. Lunau K, Wacht S, Chittka L (1996) Colour choices of naive bumble bees and their implications for colour perception. J Comp Physiol A 178:477–489. https://doi.org/10.1007/BF00190178
11. Mabry TJ, Markham KR, Thomas MB (1970) The Ultraviolet Spectra of Flavones and Flavonols. In: The Systematic Identification of Flavonoids. Springer Berlin Heidelberg, Berlin, Heidelberg, pp 41–164

12. Maia R, Eliason CM, Bitton P, Doucet SM, Shawkey MD (2013) pavo: an R package for the analysis, visualization and organization of spectral data. Methods Ecol Evol 4:906–913. https://doi.org/10.1111/2041-210X.12069
13. Makino TT, Ohashi K, Sakai S (2007) How do floral display size and the density of surrounding flowers influence the likelihood of bumble bee revisitation to a plant? Functional Ecology 21:87–95. https://doi.org/10.1111/j.1365-2435.2006.01211.x
14. Mizuno T, Sugahara K, Tsutsumi C, Iino M, Koi S, Noda N, Iwashina T (2021) Identification of anthocyanin and other flavonoids from the green–blue petals of *Puya alpestris* (Bromeliaceae) and a clarification of their coloration mechanism. Phytochemistry 181:112581. https://doi.org/10.1016/j.phytochem.2020.112581
15. Peitsch D, Fietz A, Hertel H, De Souza J, Ventura DF, Menzel R (1992) The spectral input systems of hymenopteran insects and their receptor-based colour vision. J Comp Physiol A 170:23–40. https://doi.org/10.1007/BF00190398
16. Qin Q, Tatsuzawa F, Nakane T, Kaidzuka T, Iwashina T, Mizuno T (2024) Anthocyanins and Flavonols from the Flowers of *Ranunculus* Cultivars (Ranunculaceae) and Their Color Expression. Hort J 93:114–125. https://doi.org/10.2503/hortj.QH-098
17. Rahman M, Siddika A, Bhadra B, Rahman S, Agarwala B, Chowdhury MH, Rahmatullah M (2010) Antihyperglycemic activity studies on methanol extract of *Petrea volubilis* L.(Verbenaceae) leaves and *Excoecaria agallocha* L.(Euphorbiaceae) stems. Advances in Natural and Applied Sciences 4:361–364
18. Rueda RM (1994) Systematics and evolution of the genus *Petrea* (Verbenaceae). Annals of the Missouri Botanical Garden 610–652
19. Seto H, Honda K, Komori S, Tatsuzawa F, Sasaki S (2022) Flower colors and anthocyanins of *Salvia splendens* Sellow ex Schult. and *S. coccinea*: Buc'hoz ex Etl. cultivars. Horticultural research (Japan) 21:413–423. https://doi.org/10.2503/hrj.21.413
20. Shimizu Y, Imada T, Zhang H, Tanaka R, Ohno T, Shimomura K (2010) Identification of novel poly-acylated anthocyanins from *Gynura bicolor* leaves and their antioxidative activity. Food Science and Technology Research 16:479–486. https://doi.org/10.3136/fstr.16.479
21. Spaethe J, Tautz J, Chittka L (2001) Visual constraints in foraging bumblebees: Flower size and color affect search time and flight behavior. Proc Natl Acad Sci USA 98:3898–3903. https://doi.org/10.1073/pnas.071053098
22. Tanaka T, Nakashima T, Ueda T, Tomii K, Kouno I (2007) Facile discrimination of aldose enantiomers by reversed-phase HPLC. Chemical and Pharmaceutical Bulletin 55:899–901. https://doi.org/10.1248/cpb.55.899
23. Vidana Gamage GC, Lim YY, Choo WS (2021) Anthocyanins from *Clitoria ternatea* flower: Biosynthesis, extraction, stability, antioxidant activity, and applications. Frontiers in Plant Science 12:792303. https://doi.org/10.3389/fpls.2021.792303

24. Voss DH (2002) The Royal Horticultural Society Colour Chart 2001. Journal of the American Rhododendron Society 56(1). Available at: https://scholar.lib.vt.edu/ejournals/JARS/v56n1/v56n1-voss.html
25. Zhao C, Yu Y, Chen Z, Wen G, Wei F, Zheng Q, Wang C, Xiao X (2017) Stability-increasing effects of anthocyanin glycosyl acylation. Food chemistry 214:119–128. https://doi.org/10.1016/j.foodchem.2016.07.073

Tables

Tables 1 to 4 are available in the Supplementary Files section.

Figures

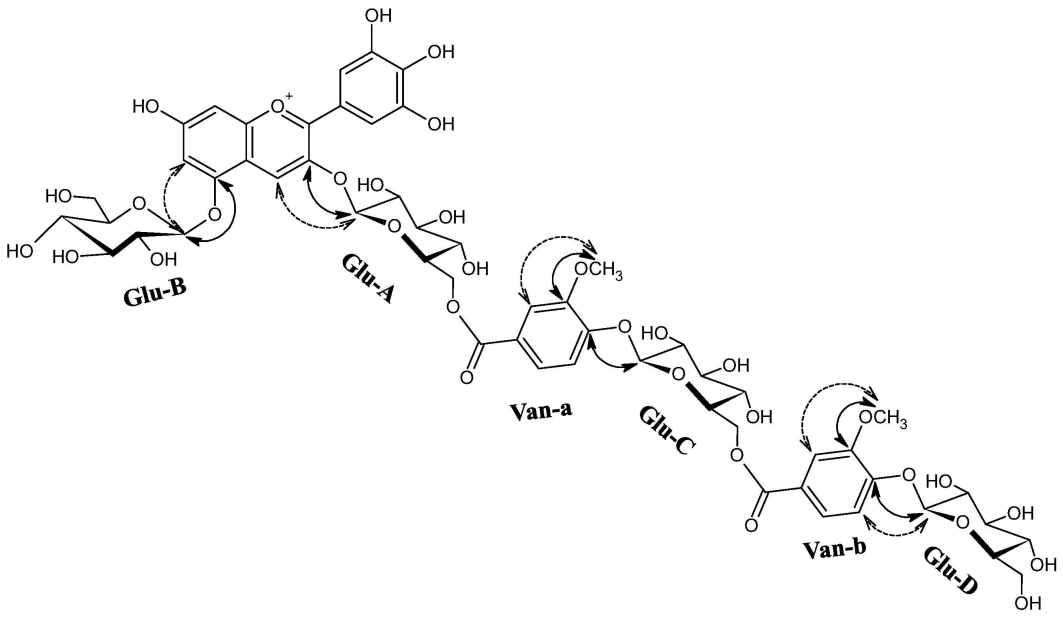

Figure 1

Chemical structure of **A1** isolated from the petals of *Petrea macrostachya*. Solid arrow = Key HMBC, Dashed arrow = Key NOESY

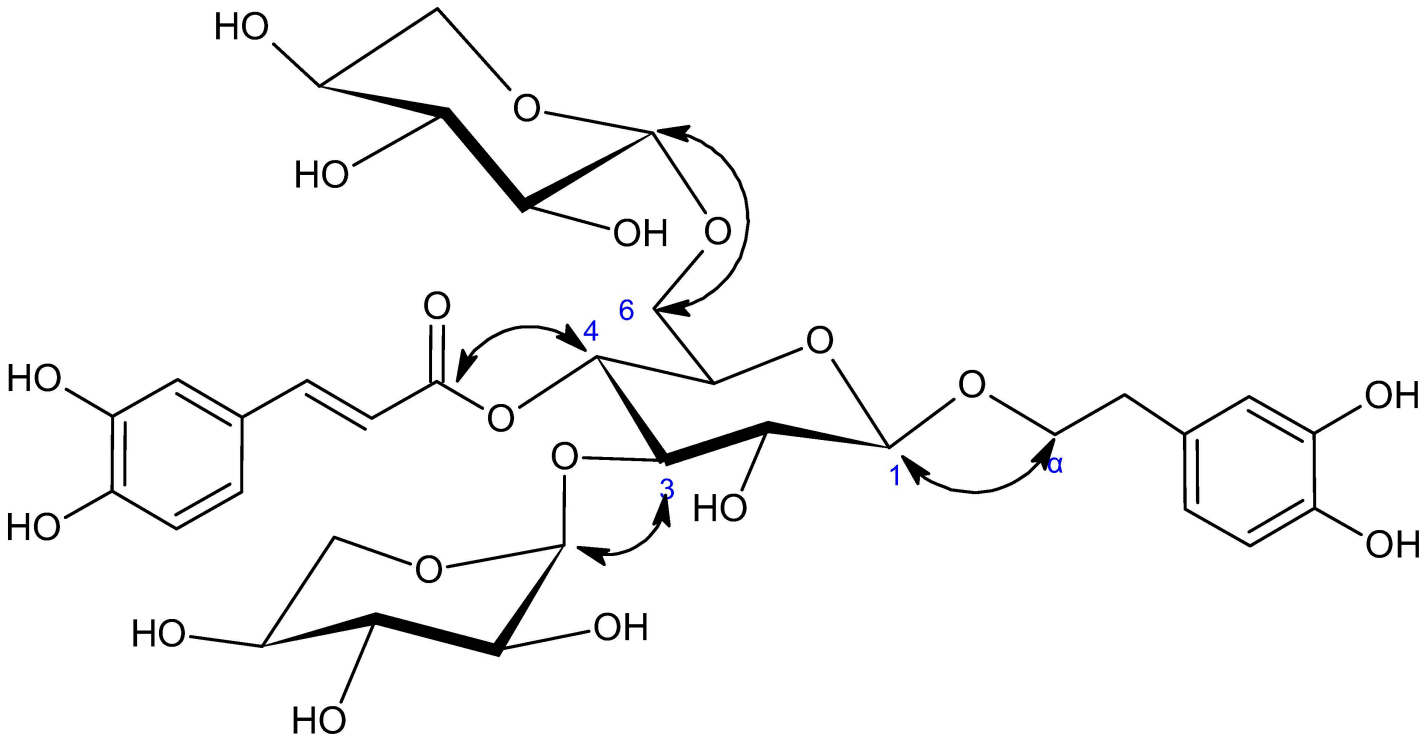

Figure 2

Chemical structure of **P4** isolated from the petals of *Petrea macrostachya*. Solid arrow = Key HMBC

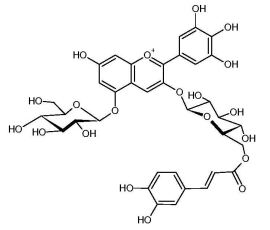

A2: delphinidin 3-*O*-(6-caffeoylglucoside)-5-*O*-glucoside

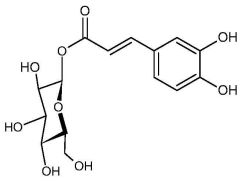

P1: *E*-caffeoylglucose

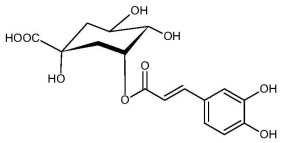

P2: neochlorogenic acid

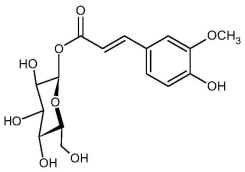

P3: *E*-feruloylglucose

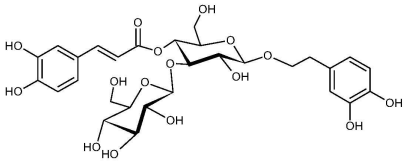

P5: plantamajoside

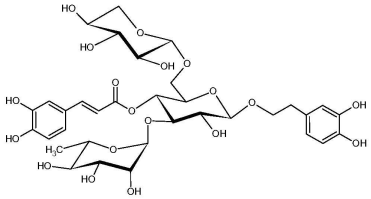

P6: forsythoside F

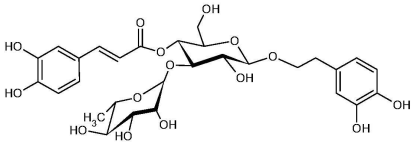

P7: acteoside (verbascoside)

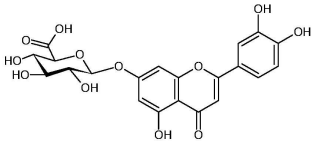

F1: luteolin 7-*O*-glucuronide

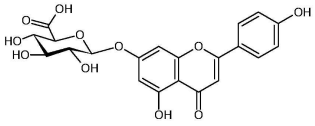

F2: apigenin 7-*O*-glucuronide

Figure 3

Chemical structures of **A2**, **P1**–**P3**, **P5**–**P7** and **F1**–**F2** isolated from the tepals of *Petrea macrostachya*

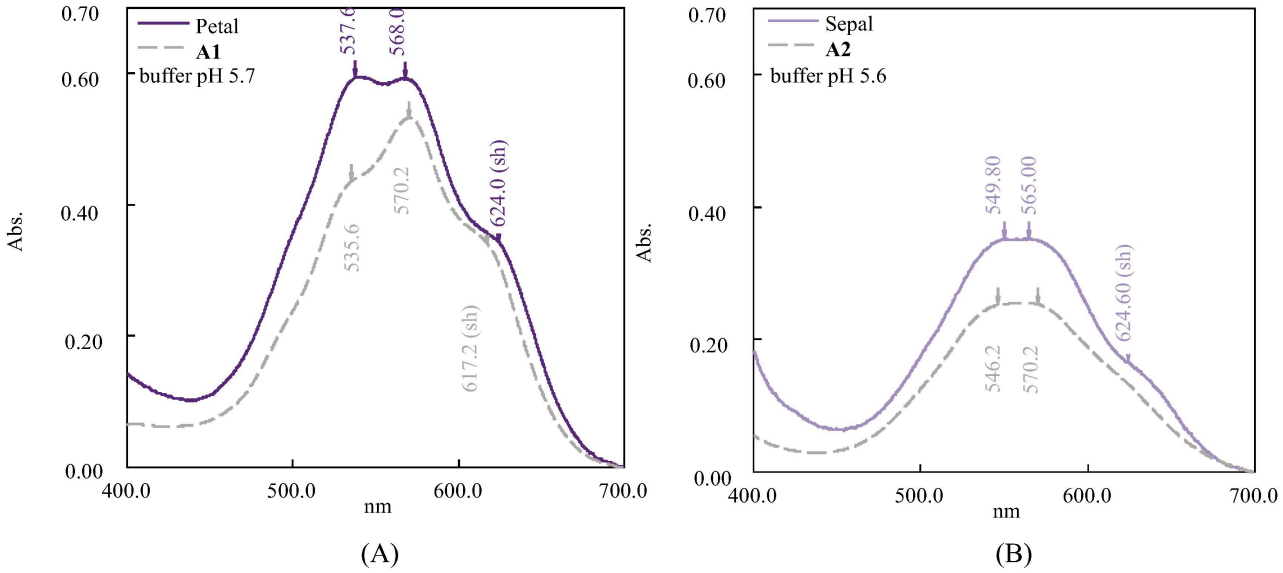

Figure 4

Comparison of the absorption spectra of *Petrea macrostachya* petals and sepals with those of *in vitro* reconstructed solutions containing the major anthocyanins. sh indicates a shoulder.

(A) Absorption spectra of intact petal and 1 mM **A1** measured in a pH 5.7 buffer solution.

(B) Absorption spectra of intact sepal and 1 mM **A2** measured in a pH 5.6 buffer solution

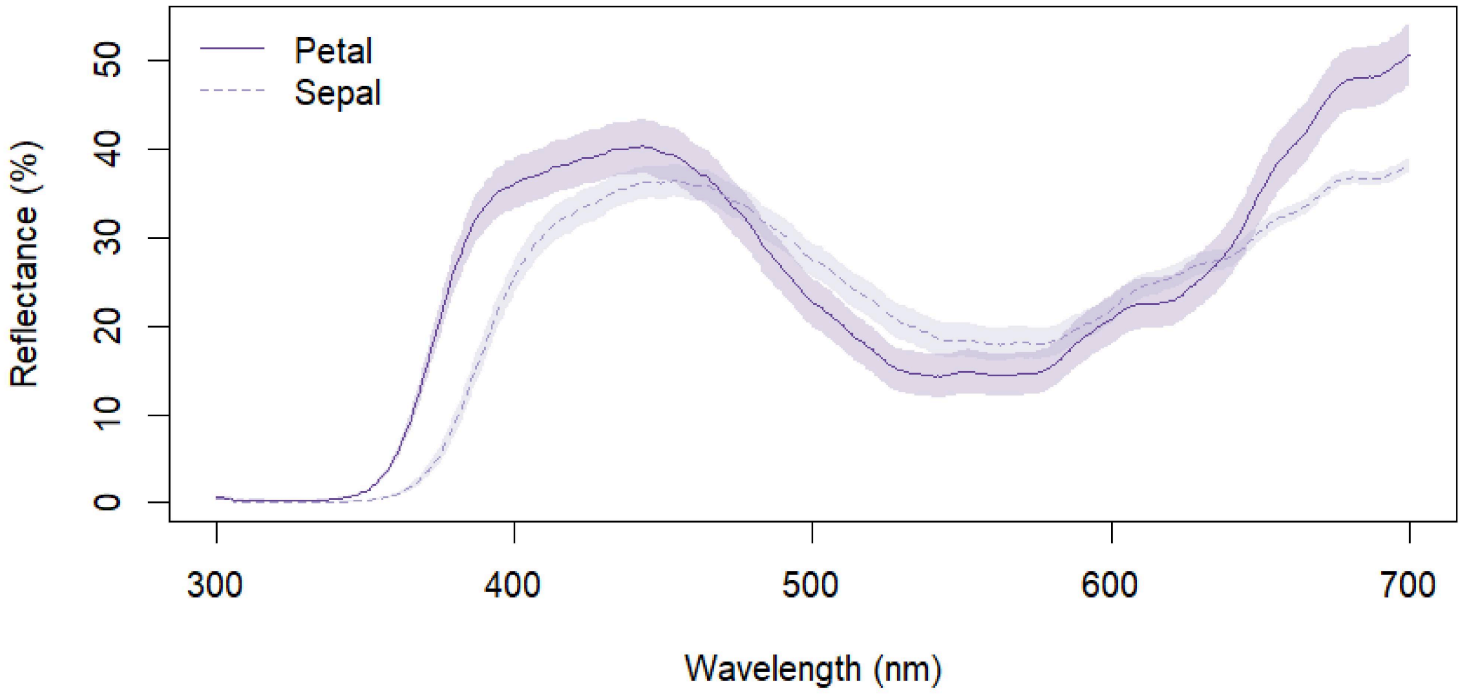

Figure 5

Reflectance spectra of the petals and sepals of *Petrea macrostachya* (petals: n=4, sepals: n=5).

The solid line represents the average reflectance of the petals, the dashed line represents the average reflectance of the sepals, and the shaded areas indicate the standard deviations

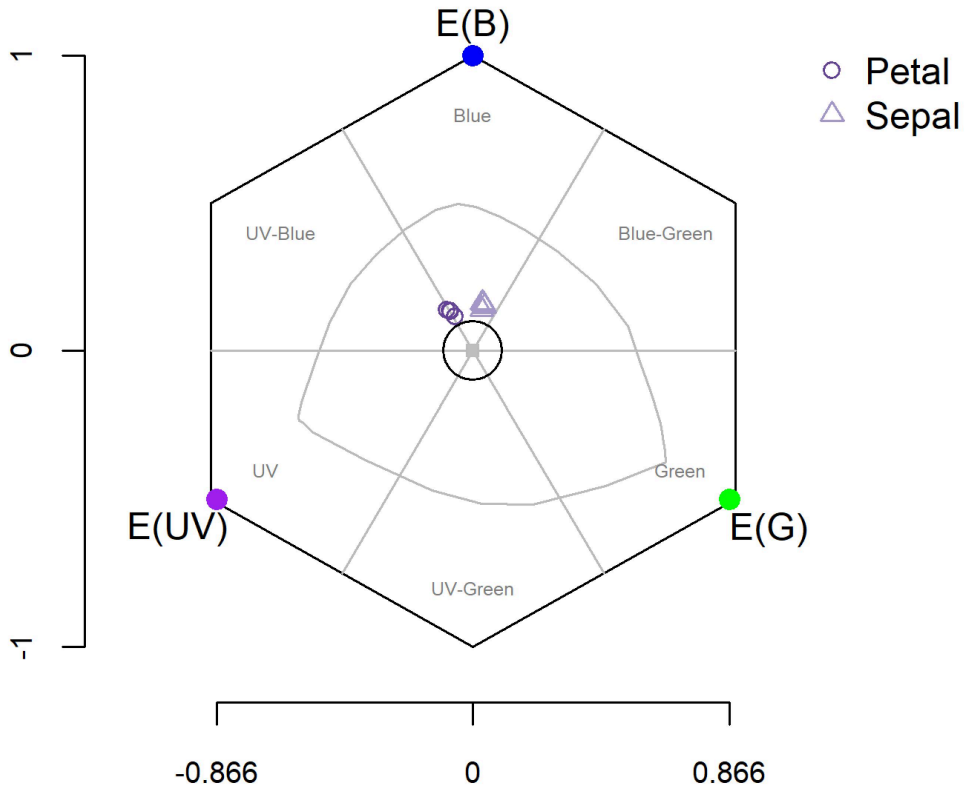

Figure 6

Color loci of *Petrea macrostachya* petals and sepals mapped in the bee color hexagon. The central circle (<0.1 hex units) encloses the uncolored category. The curved line indicates the spectral locus for *Apis mellifera* under a CIE D65 daylight irradiance spectrum, with the averaged reflectance spectrum of leaves used as the background

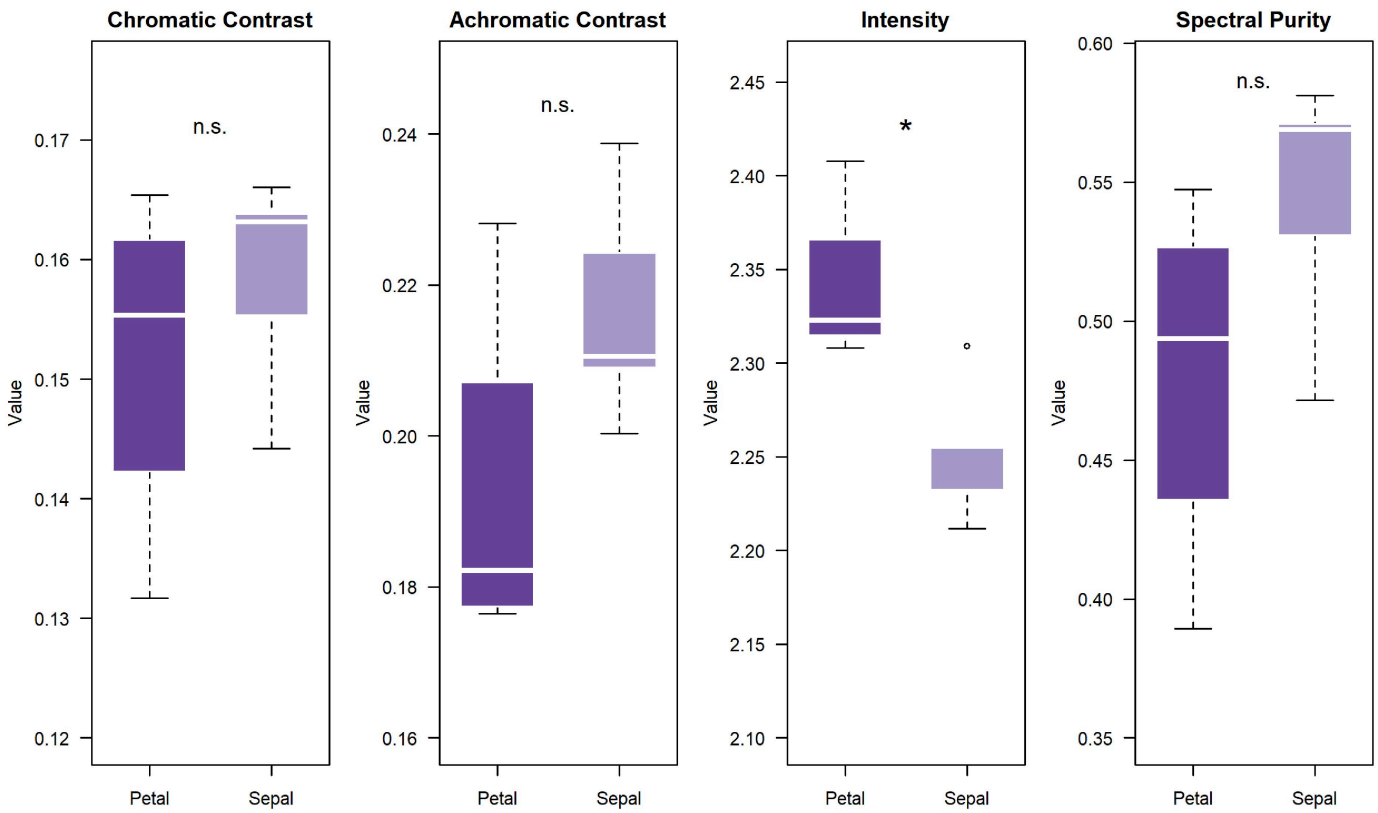

Figure 7

Color parameters of *Petrea macrostachya* petals and sepals in the bee hexagon model. Statistical comparisons were conducted using Welch's t-test ($p < 0.05$). Asterisk (*) indicate significant differences, while 'n.s.' denotes non-significant differences

Supplementary Files

This is a list of supplementary files associated with this preprint. Click to download.

- renamed5cea5.xlsx
- Supplementarydata.pdf